Cardiovascular Surgery, Hannover, Germany and Aventis Pharma Germany, Frankfurt, Germany.

IKur is supposed to be atrial selective in pigs and humans. We investigated the effects of different potassium channel blockers, such as IKur-blockers, AVE 0118, S9947 and S20951, in contrast to amiodarone (AM), dofetilide (DO), azimilide (AZ), ibutilide (IB), IKs-blocker HMR 1556, atropine (ATR), flecainide (FL), propafenone (PR), and d,l-sotalol (SO), atenolol (ATE), and esmolol (ES), on left and right atrial and ventricular refractoriness (ERP) and left atrial vulnerability (LAV) in vivo in pigs. In pentobarbital-anesthetized pigs (n = 81) atrial and ventricular ERP were measured with the S1-S2-extrastimulus-method and the QTc-time from electrocardiogram. LAV was assessed after a S2-extrastimulus applied on the left atrium.

All IKur-blockers, AVE 0118 (1mg/kg), S9947 (3mg/kg), and S20951 prolonged left stronger than right atrial ERP (54 ± 7% vs. 23 ± 7%, 56 ± 5% vs. 14 ± 2%, 29 ± 7% vs. 9 ± 2%, all $p < 0.05$) and did not change QTc-time. All IKr-blockers prolonged predominantly right vs. left atrial ERP (DO: 10μg/kg, 36 ± 4% vs. 23 ± 2%; AZ: 5mg/kg, 33 ± 2% vs. 17 ± 3%; IB: 15μg/kg, 40 ± 9% vs. 23 ± 5%, all $p < 0.05$) as did IKs-blocker HMR 1556 (1mg/kg, 16 ± 5% vs. 11 ± 5%, n.s.). AM prolonged both atria equally (30 ± 5% vs. 29 ± 5%, n.s.). ATR prolonged left atrial ERP only (12 ± 3% vs. 1 ± 1%, $p < 0.05$). Pure betablockers acted predominantly left atrial (ATE: 24 ± 5% vs. 7 ± 2%, ES, 30 ± 3% vs. 11 ± 2%, both 1mg/kg, $p < 0.05$), as did FL and PR (58 ± 15% vs. 26 ± 5%, 46 ± 5% vs. 17 ± 4%, both 1mg/kg, $p < 0.05$) while d,l-sotalol acted predominantly right atrial (1.5mg/kg, 41 ± 5% vs. 30 ± 4%, n.s.). IKur-blockers, AVE 0118, S9947 and S20951, ibutilide, and d,l-sotalol significantly decreased LAV (−100%, −100%, −82%, −53%, −53%, $p < 0.05$) in contrast to all other drugs studied.

IKur-blockers, AVE 0118, S9947, and S20951, exhibit stronger left atrial effects, not affecting ventricular repolarization. By contrast, IKr-blockers, IKs-blockers, and d,l-sotalol exert predominant right atrial and known ventricular effects. IKur-blockers inhibit atrial tachyarrhythmias stronger than all available drugs, therefore IKur-blockers seem to be promising new atrial selective antiarrhythmic drugs.

712

Reversal of tachycardia-induced atrial electrical remodeling by an L- and T-type calcium channel blocker in dogs

Kojiro Tanimoto, MD, Hideo Mitamura, MD, Narutaka Ohashi, MD, Osamu Kinebuchi, MD, Yasuo Kurita, MD, Yoko Hagiwara, MD, Shunichiro Miyoshi, MD, Motoki Hara, MD, Seiji Takatsuki, MD, PhD and Satoshi Ogawa, MD. Keio Univ School of Medicine, Tokyo, Japan.

Amiodarone has recently been demonstrated to reverse tachycardia-induced atrial electrical remodeling in dogs, but its mechanism remains to be elucidated. We hypothesized that this effect could be related to an L- and T-type Ca channel blocking property of amiodarone. To prove this hypothesis, we carried out an experimental study using efonidipine, an L- and T-type Ca channel blocker developed and commercially available as an antihypertensive agent in Japan.

Methods: In 14 dogs (11.2 ± 0.2 kg), rapid atrial pacing (RAP) at 400 bpm was given for 28 days. In 7 of them, oral administration of efonidipine (5 mg/kg/day) was started 7 days after RAP was initiated, while the other 7 dogs did not receive efonidipine. The atrial effective refractory period (ERP) was measured at 4 basic cycle lengths under autonomic blockade at baseline and every 7 days during RAP. The effect of efonidipine in the non-remodeled atria was also evaluated in another 8 dogs without receiving RAP after 14 days of the treatment.

Results: In all paced dogs, ERP decreased significantly with loss of rate adaptation by day 7 of RAP. ERP remained nearly unchanged thereafter in the dogs without receiving efonidipine. On the other hand in the dogs receiving efonidipine, after the start of the drug on day 7 of RAP, ERP increased gradually and progressively with regaining rate adaptation while RAP was continued (from 95 ± 1 to 111 ± 3 ms, $p < 0.01$). On day 28, ERP in efonidipine treated dogs became significantly longer than ERP in the dogs without receiving efonidipine ($p < 0.001$). Efonidipine did not increase ERP in dogs without undergoing RAP (from 128 ± 3 to 127 ± 3 ms, NS).

Conclusions: For the first time we have demonstrated that reversal of tachycardia-induced atrial electrical remodeling can be achieved with an L- and T-type Ca channel blocker. Clinical application of this novel strategy is strongly awaited.

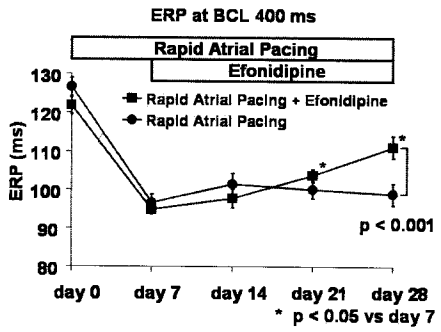

713

Predicting shapes of transmural filaments of reentrant arrhythmias in the ventricles of the heart

Alexander V. Panfilov, PhD and Kirsten H. Ten Tusscher, PhD. Univ of Dundee, Dundee, United Kingdom and Utrecht, Netherlands.

Reentry is one of the major mechanisms of ventricular arrhythmias. However, mapping studies of such arrhythmias show only rare occurrences of clear reentrant sources on the surface of the heart. This may be explained by an intramural orientation of scroll wave filaments inside the myocardium (Berenfeld, Perstov jtb, v.199:383-394,1999). Thus, prediction of filament shapes in myocardium is of great importance for interpreting experimental data on ventricular arrhythmias. In this study we propose a Method for predicting filament shape in cardiac tissue of any geometry and anisotropy. The Method is based on the 'minimal principle for rotor filaments' proposed by Wellner et al. (PNAS,v.99:8015 8018,2002). We demonstrate that this principle can be reformulated using the eikonal equation for wave propagation in the same medium in which the 3D reentry rotates. This allows us to find the stable filament position as the minimal path for a wave propagating in a given tissue. We show that this minimal path can be effectively found using wave tracing algorithms, which require knowledge of arrival times of waves initiated at the boundaries of cardiac tissue. We illustrate our approach in numerical simulations of orthotropically anisotropic cardiac tissue with several types of anisotropy and demonstrate a good correspondence of the predicted and simulated Results Because the only information necessary for using our Method is the data on arrival times, our Method can be applied for predicting filament shapes in experimental preparations without requiring any knowledge on the anisotropy of cardiac tissue.

714

Basis for the induction of phase two reentry in the Brugada syndrome: Insights from computer simulations

Flavio H. Fenton, PhD, Alfonso Bueno Orovio, MS, Elizabeth M. Cherry, PhD and Steven J. Evans, MD. Beth Israel Medical Ctr, New York, NY, Univ de Castilla-La Mancha, Ciudad Real, Spain and Hofstra Univ, Hempstead, NY.

Introduction: The Brugada syndrome is characterized by a dysfunction of sodium channels that can Result in delayed formation of the action potential dome or even complete loss of the dome during phase two in the right epicardial ventricular layers where I_{to} is large. The repolarization pattern in these cases is believed to give rise to phase two reentry; however, little is known about the specific conditions that allow or suppress its initiation.

Methods: Ionic cell models for normal epicardial, endocardial and M cells were developed in addition to two epicardial Brugada models that reproduced the action potential shape of experimentally measured human Brugada MAPs and the Luo-Rudy dynamic model with Brugada (see figures.). These models were used in 1D cables, 2D slabs, and a 3D canine ventricular model to show ST-segment elevation on ECG leads V1-V3 and to study induction of reentry by phase two.
Results: In 1D, phase two reentry can be induced when a region with loss of dome is adjacent to a region with a delayed dome, independent of stimulation site. In 2D, phase two reentry can be initiated when three regions (lost dome, delayed dome, and normal) are present, and sustained reentry initiates following an activation from any stimulus site outside the normal tissue. In 3D, sustained phase two reentry requires taking into account the different resistivity between the epicardial and M cell layers.
Conclusions: The inducibility of phase 2 reentry depends on a number of factors, including I_{to} and resistivity distribution, rate and direction of stimulation, and most importantly, the shape of the late plateau, the action potential duration with loss of dome, and the rate of sodium inactivation.

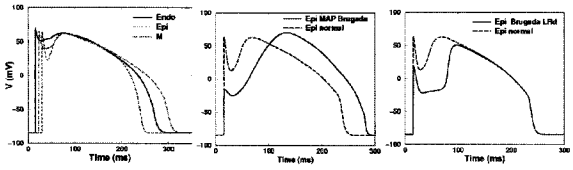

715

Modelling vortices of electrical waves in mice hearts

Jacques Beaumont, PhD and Jason D. Bayer, BSc. Upstate Medical Univ of SUNY, Syracuse, NY.

Background: the mouse is the most practical and economical model to carry out genetic manipulations aiming at investigating the molecular mechanisms underlying cardiac death. However, a difficulty currently encountered with such model is that either spontaneous or induced arrhythmias self terminate shortly after initiation.
Objective: Elucidate the cause of arrhythmias self termination in normal and transgenic mice myocardiums.
Method: We simulate impulse propagation in a realistic model of the mouse heart. The reconstruction is based on a fusion of X-ray and confocal imaging modalities. The Resulting geometry is meshed with 5 million elements, over which excitation is described with a detailed membrane model. Simulations are performed on massively parallel computers.
Results: The heart reconstruction (8 microns resolution) includes trabeculations, papillary muscles, and a representation of the three-dimensional cardiac fibers arrangement (5 microns resolution) in the entire heart including the above mentioned regions. Vortex activity in the heart is initiated with two point source stimuli. One at the apex and the other one in the free wall of the left ventricle 3 mm above the apex. Adjusting timing between the two stimuli and the circumferential position of the second stimulus vortices are initiated at different locations in the heart. In the majority of cases vortices drift toward the base and terminate when they collide with the latter. Occasionally they stabilize for about 1 second in highly convoluted regions of the heart. Mutations Resulting in an APD prolongation reduce the time of sojourn in stabilizing sites.
Conclusion: self-termination of arrhythmias is the Result of vortex drift. Functional anchoring may occasionally occur, but at this time we cannot conclude as to whether it may be permanent

716

Negative VEP affects activation during diastolic stimulation in the rabbit ventricles

Mary M. Maleckar, BS and Natalia A. Trayanova, PhD. Tulane Univ, New Orleans, LA.

To further characterize the mechanisms of defibrillation, it is necessary to understand responses to shocks during diastole in the 3D volume of the ventricles. However, the few experimental studies that examined diastolic responses conducted measurements on the epicardium and, recently, on a transmural surface of the LV wall. This study investigates myocardial response to shocks in diastole throughout the volume of the rabbit ventricles using a realistic computational model of stimulation/defibrillation.
Methods: An anatomically accurate 3D bidomain model of the rabbit ventricles was subjected to shocks in diastole. Truncated exponential, 8ms long shocks of strengths in the range 1.5–18.75V/cm were administered via parallel-plate electrodes submerged in the surrounding perfuseate.
Results: Total activation time as measured from the start of the shock varied from 26 to 55ms, rapidly decreasing and then slowly increasing as shock strength increased (figure, left panel). Early activation in the LV base was observed for lower (1.5–3V/cm) but not for higher shock strengths. During the shock, the pattern of transmural activation was similar for all mid-range shocks (6–18.75V/cm) and revealed deceleration of the propagating wavefront. We hypothesized that the shock-induced negative VEP caused activation delay and thus, paradoxical increase in activation times for higher shock strengths. Examination of VEP revealed an increase in negative VEP predominantly in the septum and the LV free wall with increase in shock strength (see right panel). The increase in negative VEP inhibited basal activation and slowed propagation for mid to high strength shocks.
Conclusion: During shocks in diastole, negative VEP causes propagation delay for higher strength shocks, Resulting in an unexpected increase in total activation time.

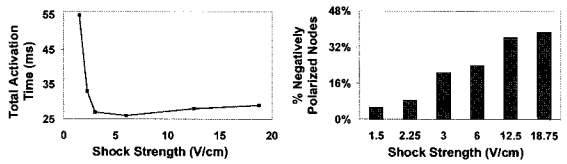

717

Analysis of *SCN5A* gene mutation in Japanese patients with arrhythmia

Takeru Makiyama, Takahiro Doi, Seiko Ono, Atsushi Kobori, MD, PhD, Tomonori Ninomiya, Keiko Tsuji, Masaharu Akao, Makoto Takano, Wataru Shimizu, MD, PhD, Naomasa Makita and Minoru Horie, MD, PhD. Kyoto Univ Graduate School of Medicine, Kyoto, Japan, National Cardiovascular Ctr, Suita, Japan, Hokkaido Univ Graduate School of Medicine, Sapporo, Japan and Shiga Univ of Medical Science, Seta, Japan.

Objective: *SCN5A* gene encodes the α-subunit of voltage-gated cardiac Na channel, which plays an important role in heart excitation/contraction. Mutations in *SCN5A* cause distinct and inherited types of arrhythmias: type 3 long QT syndrome (LQTS3), Brugada syndrome (BS), idiopathic ventricular fibrillation (IVF), cardiac conduction disturbance (CCD) and even overlap of them. We analyzed *SCN5A* gene mutations and polymorphisms among Japanese patients with inherited arrhythmia.
Methods: Genomic DNA was obtained from 150 probands of arrhythmia patients (congenital and acquired LQTS, BS, IVF, CCD and overlap syndrome) and 110 normal controls. Genetic variants in *SCN5A* were screened by using a Denaturing High Performance Liquid Chromatography, and were subsequently determined by a direct DNA sequencing. Several mutations were engineered into the hH1 clone by using a site-directed mutagenesis Method, then expressed in HEK 293 cells, and were studied by a whole-cell mode of patch clamp Method.
Results: Nine *SCN5A* mutations (5 novel and 4 reported) were identified (5 in LQTS, 2 in BS, and 2 in overlap syndrome), and were not seen in 220 alleles of normal controls. One novel single nucleotide polymorphism (SNP), L1988R, was also found in 6 patients (0.04%), and in 2 controls (0.02%). Functional assay was conducted in 3 of 5 novel mutations: N1774D mutation was identified in a newborn LQTS, so-called near Sudden Infant Death Syndrome case. The N1774D mutant displayed a significant increase in the late Na current, and simultaneously, it caused a